Experimental campaign and modeling of a low-capacity waste heat recovery system based on a single screw expander

Adriano Desideri[1*], Martijn Van Den Broek[2,3], Sergei Gusev[2], Vincent Lemort[1], Sylvain Quoilin[1]

[1] University of Liège, Aerospace and Mechanical Engineering Department, Liège, Belgium 4000
adesideri@ulg.ac.be, squoilin@ulg.ac.be, vincent.lemort@ulg.ac.be

[2] Ghent University, Department of Industrial System and Product Design, Kortrijk, Belgium
sergei.gusev@ugent.be

[3] Ghent University, Department of Flow Heat and Combustion Mechanics, Ghent, Belgium
martijn.vandenbroek@ugent.be

* Corresponding Author

ABSTRACT

This paper presents an experimental characterization of an 11 kWe single screw expander modified from a standard compressor and integrated into an organic Rankine cycle (ORC) test facility using Solkatherm as working fluid. A total of 62 steady-state points are collected over a wide range of operating conditions to evaluate the expander and the system performance by changing the rotational speed, the pump frequency and the cooling condenser flow rate. The maximum expander isentropic efficiency and generated power are respectively 64.78% and 7.8 kWe. A maximum cycle efficiency of 9.8% is reached for an evaporating temperature of 108°C and a condensing temperature of 27.5°C. A low order semi-empirical model of the expander is derived based on the experimental data. Performance curves for the ORC unit components are implemented and used to develop a steady-state model of the ORC unit. The steady-state model of the whole system is then validated against experimental data.

1. INTRODUCTION

The increasing concern over energy shortage and global warming has raised a growing interest in low grade heat recovery from industrial processes (IEA (2010)). Heat recovery technology represents a viable approach in reducing the operating cost for industrial facilities by increasing the energy productivity (DOE (2008)). Among other technologies, organic Rankine cycle (ORC) power systems have been proven to be a mature and viable technology for waste heat recovery applications (Verneau (1979) David et al. (2011) Moynihan (1982)). ORC units stand out for their reliability and cost-effectiveness (Angelino et al. (1984)). The characteristics of the ORC fluids allow for micro-scale units (3 - 20 kW_E) and low temperature (90 - 150°C) applications (Davidson (1977) Walraven et al. (2013)). The expander is a key element in an ORC system. In the micro power range, positive displacement machines present characteristics that make them a privileged choice over turbo-generators: low flow rate, low rotational speed, high pressure ratio (Persson (1990)). In addition, displacement machines can handle two-phase flow, condition that can appear at expander outlet when operating with "wet fluids". However, in the micro power range, commercial expanders are still in an early stage of development and are therefore not cost-competitive yet. A common solution to obtain a cost-effective expansion machine is to modify an existing compressor (Quoilin et al. (2013) Lemort et al. (2011) Declaye et al. (2013)).
Among the volumetric expander technologies, single screw expander represents a novel and promising candidate for ORC sytems in the micro power range. Recent studies have reported the performance of in-house built single screw expander for low power capacity. Wang et al. (2011) presented a 5 kWe machine with an isentropic efficiency of up to 59%. He et al. (2013) built and tested a 22 kWe single screw expander reaching a maximum isentropic efficiency of 55% at 2800 rpm. Wang et al. (2013) analyzed the influence of the gaterotor/shell and the screw/shell gap by building and testing three different single screw expanders. From this analysis they conclude that the machine with a medium gap characteristic achieved the best performance with an output power of 5 kWe and an isentropic efficiency of 60%. The working fluid employed in the cited works is compressed air which is not commonly used in waste heat recovery

plants. Experimental data of such machines operating with organic fluids is lacking at the present time. A preliminary experimental comparison of organic working fluids on the same test bench presented in this work is reported in Sergei et al. (2014). In this paper, an organic Rankine cycle test facility designed to test an 11 kWe single screw expander, is presented in detailed. A set of experimental tests using Solkatherm as working fluid are analyzed. A critical analysis of the experimental results is then presented, with the derivation of empirical performance curves for each components. These empirical models are implemented in the Modelica language (Mattsson and Elmqvist (1997)) and interconnected to build the complete model of the ORC system (Desideri et al. (2013)). In this paper a more complete data set of experimental tests is reported. The data are used to develop and validate a semi-empirical model of the single screw expander. A deterministic model of the considered single screw expander is described in Ziviani et al. (2014). The obtained expansion machine model together with the performance curves for the other ORC components is used to develop a steady-state ORC system. A validation of the overall steady-state ORC model is finally presented.

2. EXPERIMENTAL SET-UP

A front view of the ORC test rig and a schematic layout of the test bench are shown in figure 1a and 1b. The system has a nominal power of 11 kWe and is based on a regenerative cycle. Solkatherm is selected as working fluid for ease of use, non flammability and thermal stability up to 190°C. The expander is a single screw compressor adapted to run in expansion mode with a built-in volume ratio of 6 (Ziviani et al. (2014)). MOBIL EAL ARCTIC 68 oil is added in the cycle, with a 3.23 % of the total mass of working fluid, to lubricate the rotor. The bearings of the expander are lubricated through a by-pass pipe directly from pump outlet to the expander as shown in figure 1b. The expander is connected to an asynchronous machine whose speed is controlled by means of a four quadrant inverter. A vertical variable speed multistage centrifugal pump, driven by an inverter, is used to circulate the fluid through the system. The evaporator, recuperator and condenser are brazed plate heat exchangers composed by 150 plates each. A liquid receiver installed at the outlet of the condenser allows to control the charge of working fluid in the system.

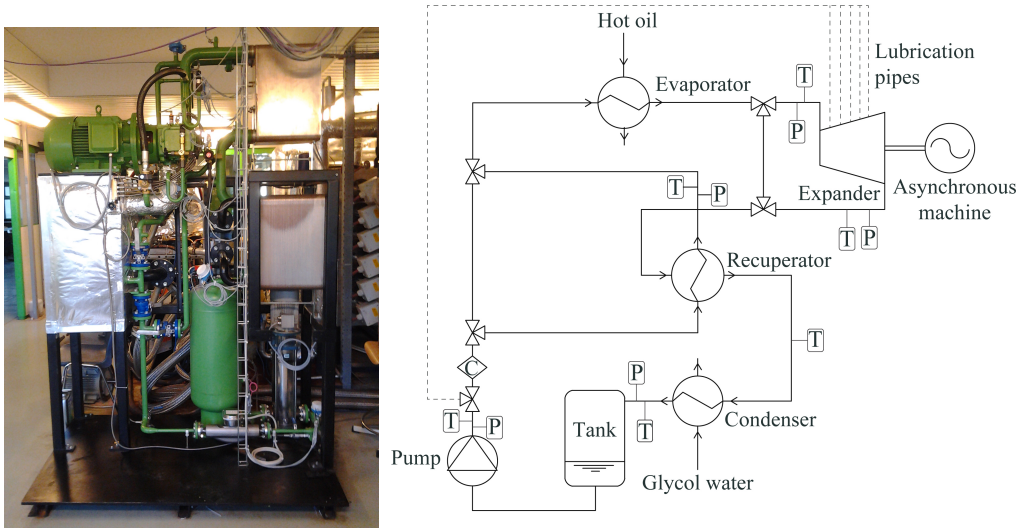

(a) Front view of the ORC test rig **(b) Schematic layout of the ORC test rig**

Figure 1: ORC test facility

2.1 Heating loop

The thermal energy source is provided by an electrical boiler with a maximum power of 250 kW_T. Therminol66 is selected as heating fluid and is pumped through the evaporator. A proportional integer (PI) controller is implemented to maintain the temperature of the oil at the inlet of the evaporator constant during transient in the ORC test rig (e.g. change of ORC pump rotational speed).

2.2 Cooling Loop

A variable flow rate of glycol water, 32% vol. ethylene glycol, is used as heat sink to cool down the working fluid in the condenser. The thermal energy absorbed by the cooling fluid is rejected in the ambient by means of an air cooler. A by-pass of the air cooler allow controlling the condenser temperature by means of an adjustable solenoid valve.

2.3 Data Aquisition System

Absolute pressure sensor (APS) and resistance temperature detectors (RTD) at the inlet and at the outlet of the different components allow the determination of the energy balance for each component and the management of the plant. The Solkatherm mass flow rate is measured by means of a Coriolis flow meter (CFM) installed at the turbo-pump outlet. The cooling loop is equipped with two RTDs to measure the temperature of the cooling fluid at the inlet and at the outlet of the condenser and an ultrasonic flow-meter is used to measure the flow rate of glycol water. In the thermal energy circuit, the temperature of Therminol66 is measured at the inlet and at the outlet of the evaporator and a pressure difference transmitter is used to calculate the oil mass flow. The electrical power at the generator outlet is measured by means of a wattmeter. The data acquisition system is done with a PLC, and a Microsoft PC with LabView is used for data visualization. The characteristics of the measurement devices are reported in table 1.

Variable	Device type	Range	Uncertainty
SES36 mass flow	CFM	0 kg/s to 1.8 kg/s	± 0.09%
T (ORC)	RTD	50°C to 300°C	± 0.2°C
T (heat sink)	RTD	0°C to 150°C	± 0.2°C
T (heat source)	RTD	30°C to 350°C	± 0.2°C
p	APS	0 bar to 16 bar	± 0.016 bar
El. Power	Wattmeter	0 to 100 GW	± 0.1%

Table 1: Range and accuracy of the measurement devices

3. EXPERIMENTAL INVESTIGATION

In total 62 steady-state points are collected, covering a wide range of operating conditions. The cycle operates between a maximum oil temperature of 125°C and a minimum glycol-water temperature of -0.6°C. The Solkatherm flow is imposed by varying the pump rotational speed, the evaporating pressure is controlled by adjusting the expander rotational speed and the condensation pressure is imposed by adjusting the cooling flow rate in the condenser. On-line signal plotting is used to ensure that a steady state condition is achieved before any change is imposed to the system. The minimum and maximum performance achieved during the measurement campaign are reported in table 2.

Performance	η_{cycle} (%)	$\varepsilon_{is,exp}$ (%)	$\varepsilon_{is,P}$ (%)	$p_{su,exp}$ bar	$r_{p,exp}$ -	$T_{su,exp}$ (°C)	ΔT_{sc} (°C)	ΔT_{sh} (°C)	PP_{ev} (°C)	PP_{cond} (°C)	ΔP_{LP} (bar)	ΔP_{HP} (bar)
Min	0.2	13.25	12.3	4.5	3.12	119.3	9	1	0.1	0.1	0.06	$0.4 \cdot 10^{-3}$
Max	9.8	64.78	20	10.2	10.97	125	26	29	0.7	1	0.17	0.09

Table 2: Min/Max performance achieved during measurement campaigns. η_{cycle} cycle efficiency, $\varepsilon_{is,exp}$ isentropic effectiveness of the expander, $\varepsilon_{is,P}$ effectiveness of the pump, $p_{su,exp}$ pressure at the inlet of the expander, $r_{p,exp}$ expander pressure ratio, $T_{su,exp}$ temperature at the outlet of the evaporator, ΔT_{sc} condenser subcooling, ΔT_{sh} evaporator super-heating, PP_{ev} and PP_{cond} evaporator and condenser pinch point, ΔP_{LP} and ΔP_{HP} low and high pressure drop respectively.

The very low pinch point values in the evaporator and in the condenser are due to a large exchange area, which entails a high heat exchange effectiveness. A significant value of the subcooling is registered during the tests. It can be explained with the presence of non-condensable gases due to the sub-atmospheric value of the Solkatherm condensing pressure for some of the operating conditions. A relatively low pump performance is recorded, with a maximum isentropic efficiency of 20%. It is noteworthy that a maximum cycle efficiency of 9.8% is reached despite the poor pump performance and the presence of non-condensable gases.

3.1 Expander performance

Figures 2a and 2b show the evolution of the expander isentropic efficiency and the generated expander power as a function of the pressure ratio with a constant inlet expander temperature of 125°C and a fixed discharge pressure of 1.1 bar for two rotational speed 2000 and 3000 rpm. A total of 41 and 21 points have been collected for a rotational speed of 3000 and 2000 rpm respectively. The isentropic efficiency is calculated as:

$$\varepsilon_{s,exp} = \frac{\dot{W}_{shaft}}{\dot{m} \cdot (h_{su} - h_{ex,s})} \quad (1)$$

The enthalpies are computed using CoolProp, an open-source thermophysical properties database (Bell et al. (2014)).

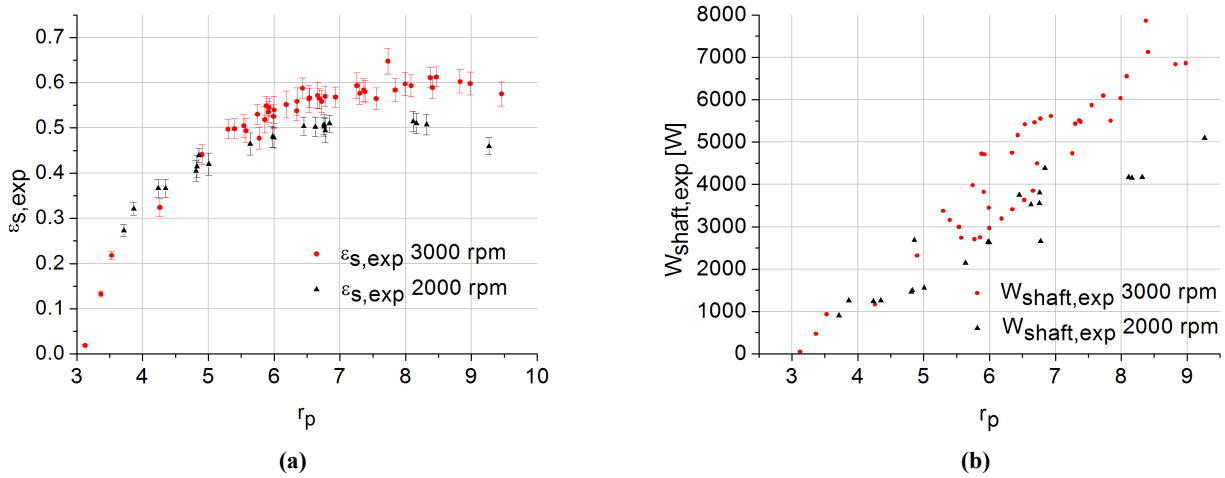

Figure 2: (a) Expander effectiveness and (b) expander shaft power vs pressure ratio for two rotational speed, 2000 rpm in red and 3000 rpm in black, for a constant inlet expander temperature of 125°C and a fixed discharge pressure of 1.1 bar.

As shown in figure 2a, the isentropic efficiency trend for the two considered rotational speeds is characterized by a maximum that is due to a fixed built-in volume ratio of the expander. The pressure ratio applied to the expander differs from the optimal pressure ratio corresponding to the built-in volume ratio for most of the tests. This yields to over/under expansion losses whose impact is minimized when the pressure ratio matches the internal pressure ratio of the expander. For a pressure ratio values ranging from 6.5 to 9, the isentropic efficiency at 3000 rpm is about 11% higher than at 2000 rpm. For lower pressure ratio this difference tends to disappear. These results are in line with the numerical results of Lemort et al. (2011) according to which at low rotating speed and high pressure ratio the impact of leakages on the performance of the expander is predominant. The maximum expander isentropic efficiency ranges from 51% at 2000 rpm to 64.78% at 3000 rpm. The pressure ratio that maximizes the isentropic efficiency ranges from 6.84 at 2000 rpm to 7.73 at 3000 rpm. This shift can be due to the relative impact of leakages losses as explained above. At high pressure ratios, under-expansion occurs, as described in Lemort et al. (2011): the built-in volume ratio is too low for the imposed expansion ratio and the efficiency decreases. In figure 2b the shaft power of the expander is plotted as a function of pressure ratio for the two analyzed rotational speed. The trend of the shaft power differs from the one of the isentropic efficiency, resulting in a monotonically increasing function of the pressure ratio. The scattering characterizing the plot is due to the variations of additional operating conditions not displayed in the plot, such small variations on the inlet pressure. A maximum power of 7.8 kW_E is reached for a pressure ratio of 8.5.

4. STEADY-STATE MODELING

4.1 Expander

Based on the collected experimental data a steady state semi-empirical expander model is developed. The expander can be modeled by its effectiveness and its filling factor, if heat losses to the environment are neglected (Declaye et al. (2013)). The expander effectiveness and the filling factor are defined in equations 1 and 2.

$$\varphi = \frac{\dot{m}}{\rho_{su,exp} \cdot (V_s N_{rot})} \tag{2}$$

The effectiveness of the expander can be fitted with an expression by carefully selecting the input variables. In this case the selected variables are the expander inlet pressure, $p_{su,exp}$, the expander rotational speed, $N_{rot,exp}$ and the expander pressure ratio, r_p, because they are representative of the overall boundary conditions of the machine. The mathematical form of the semi-empirical equation is selected to fit the trend of the expander efficiency as a function of the pressure ratio as shown in figure 2a. The expression was proposed by Declaye et al. (2013) and it is written:

$$\varepsilon_{is,exp} = y_{max} \cdot (\xi \cdot arctan(B \cdot (r_p - r_{p,0}) - E \cdot (B \cdot (r_p - r_{p,0}) arctan(B \cdot (r_p - r_{p,0})))))) \tag{3}$$

with:

$$B = \frac{\delta}{\xi \cdot y_{max}} \tag{4}$$

$$E = \frac{B \cdot (r_{p,max} - r_{p,0}) - tan\frac{\pi}{2\xi}}{B \cdot (r_{p,max} - r_{p,0}) - arctan(B \cdot (r_{p,max} - r_{p,0}))} \tag{5}$$

where the parameters $r_{p,0}$, δ_n, ξ, $y_{max,n}$ and $N_{rot,n}$ have a mathematical meaning described in table 3. The parameters are expressed as a linear regression of the three selected input variables using seven empirical coefficients a_x and b_x as shown in equations 7 - 10. The input variables are defined in non-dimensional form as shown in equation 6.

$$r_p^* = \frac{r_p - 4}{4}; \quad N_{rot}^* = \frac{N_{rot} - 3000}{3000}; \quad p_{su,exp}^* = \frac{p_{su,exp} - 10}{10} \tag{6}$$

$$r_{p,0} = r_{p,0,n} + a_0 \cdot N_{rot}^* \tag{7}$$

$$\delta = \delta_n + a_1 \cdot p^* + a_2 \cdot N_{rot}^* \tag{8}$$

$$r_{p,max} = r_{p,max,n} + a_3 \cdot p^* + a_4 \cdot N_{rot}^* \tag{9}$$

$$y_{max} = y_{max,n} + a_5 \cdot p^* + a_6 \cdot (N_{rot}^* - N_{rot,n}^*)^2 \tag{10}$$

with

$$N_{rot,n}^* = \frac{N_{rot,n} - 3000}{3000} \tag{11}$$

The empirical coefficients are identified using the experimental data with a robust regression method Huber (1992). The empirical coefficients values are reported in table 3. A coefficient of determination, R^2, of 91.3% is obtained for the isentropic efficiency. In figure 3 a 3D map of the isentropic efficiency, computed with the developed empirical equation, is shown as a function of pressure ratio and rotational speed for an inlet pressure of 8 bar. The maximum isentropic efficiency for the screw machine is about 10 points lower than the one exhibits by scroll machines (Declaye et al. (2013)). On the other hand the screw machine presents its optimal performance for a pressure ratio significantly higher than the scroll expander, as demonstrated in Quoilin et al. (2012). This is a non-negligible advantage since it makes the screw expander more adapted to the typical operating conditions of low to medium temperature ORC power systems.

As the swept volume V_s is not known, the group $\varphi \cdot V_s$ is modeled rather than the filling factor with equation 12 assuming a swept volume of one.

Performance	Description	Value
$r_{p,0}$	x-intercept of the efficiency curve as a function of the pressure ratio	3.076
δ_n	Slope of the efficiency curve close to the x-intercept	0.7924
ξ	Parameter setting the shape of the efficiency curve	1.213
$y_{max,n}$	Maximum efficiency for the reference conditions	0.592
$r_{p,max,n}$	Optimal pressure ratio for the reference conditions	10
$N_{rot,n}$	Optimal rotational speed for the reference conditions	3547
Empirical parameters:		
$a_0 = 0$; $a_1 = 0.8411$; $a_2 = 8.347$; $a_3 = 3$; $a_4 = 3$; $a_5 = 0.023383$; $a_6 = 0.4827$		

Table 3: Expander model parameters

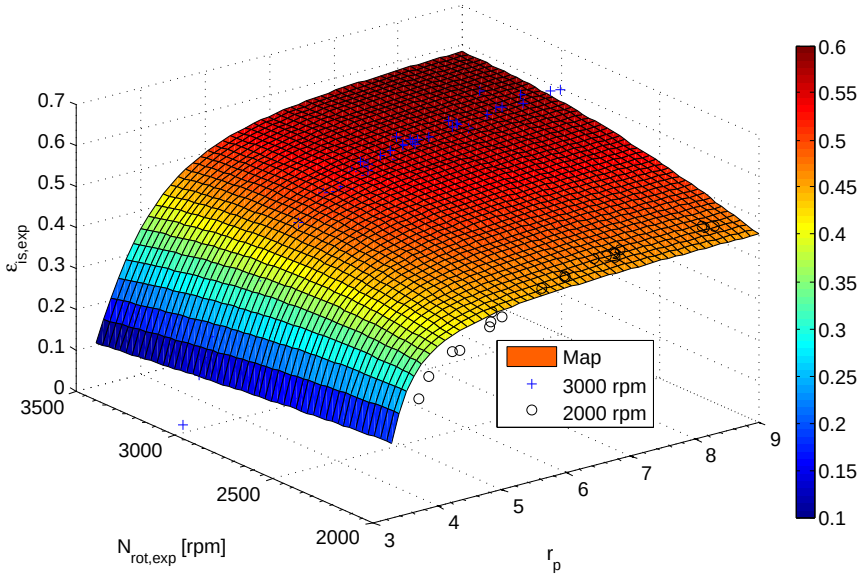

Figure 3: 3D map of expander isentropic efficiency for an inlet pressure of 8 bar plotted together with the collected experimental data

$$\varphi \cdot V_s = \frac{\dot{m}_{pred}}{N_{rot} \cdot \rho_{su,exp}} \tag{12}$$

where $\dot{m}_{pred}$ is the mass flow entering the expander predicted with a second order polynomial law with cross terms as a function of the non-dimensional expander inlet pressure, $p^*_{su,exp}$, and expander rotational speed $N^*_{rot,exp}$. The obtained coefficient of determination has a value of 94.22%.

4.2 Heat Exchanger

The heat exchangers are modeled by 4 heat transfer coefficients (three for the liquid, two-phase and vapor zones on the refrigerant side and one for the secondary fluid side). Inconsistency during the transition between two heat transfer coefficients is avoided by means of a smooth transition function. The recuperator model is based on the condenser and the evaporator model considering a single fluid phase on both side of the exchanger. Pressure drops are assumed to be lumped on the vapor lines. As reported in tables 1 and 2, for most of the data points, the heat exchanger pinch points are smaller than the sensor uncertainty. This is due to the oversizing of the heat exchangers, and it impedes properly validating a heat transfer model since any heat transfer coefficient with a sufficiently high value will predict the heat exchanger performance within the sensor accuracy.

4.3 Pressure Drop

In an ORC power unit, pressure drops mainly occur in the heat exchangers. In this work it is assumed that pressure drops are lumped in the lowest vapor density part of both low and high pressure lines. This approach is valid when pressure drops are relatively small (table 2) and facilitates the convergence of the numerical iteration process (Quoilin (2011)). Pressure drops are modeled as a function of a linear and a quadratic term, accounting for laminar and turbulent pressure drops, as shown in equation 13. The parameter k, in the linear pressure drop equation, and the valve throat area A, in the quadratic pressure drop expression, are identified with a linear regression based on the experimental data. Their values together with the relative coefficient of determination are collected in table 4.

$$\Delta p = \Delta p_{\text{linear}} + \Delta p_{\text{quadratic}}; \quad \Delta p_{linear} = k \cdot \dot{V}; \quad \Delta p_{\text{quadratic}} = \frac{1}{A^2} \cdot \frac{\dot{m}^2}{2 \cdot \rho} \tag{13}$$

Pressure drop	k	A	R^2
Δp_{HP}	-7.80690436E+05	0.0002523	26.93%
Δp_{LP}	258293	0.001508	47.39%

Table 4: Pressure drop model parameters

4.4 Pump

In order to model the turbo-pump installed in the ORC system, an expression for the effectiveness and for the delivered mass flow rate is fitted based on some selected input variables. The effectiveness is expressed as a function of the non-dimensional pressure ratio over the pump, $r^*_{\text{p,P}}$, and the non-dimensional pump frequency, f^*_{P}, with a coefficient of determination of 79.86 %. The mass flow rate is expressed as a function of the non-dimensional pump frequency f^*_{P} with a coefficient of determination of 86.68 %. The low accuracy of the obtained correlations is due to the low repeatability of the pump performance during the experimental test. The isentropic efficiency equation is reported in equation 14 and the relative parameter values are shown in table 5.

$$\varepsilon_{\text{is,P}} = A_0 + A_1 \cdot f^*_{\text{P}} - A_2 \cdot f^{*2}_{\text{P}} - A_3 \cdot r^*_{p,P} + A_4 \cdot r^{*2}_{p,P} + A_5 \cdot f^*_{\text{P}} \cdot r^*_{p,P} \tag{14}$$

where

$$r^*_{\text{p,P}} = \frac{r_{\text{p,P}} - 9}{9} \qquad ; f^*_{\text{P}} = \frac{f_{\text{P}} - 30}{30} \tag{15}$$

Parameter	Value
A_0	1.64002163E-01
A_1	2.61635282E-01
A_2	3.93078704E-01
A_3	7.82556670E-03
A_4	1.91223439E-05
A_5	5.89131488E-02

Table 5: Isentropic pump efficiency model parameters

5. ORC SYSTEM MODEL VALIDATION

The steady state models of the different ORC system components, derived from the experimental data, are coupled together to model the ORC power unit. The derived steady-state model is validated against the experimental values. In figure 4 the prediction of the net output power of the ORC unit model, defined in equation 16, is plotted versus the experimental values for 7 points selected to cover a broad range of operating conditions.

$$\dot{W}_{\text{orc}} = \dot{W}_{\text{shaft,exp}} - \dot{W}_{\text{P}} \tag{16}$$

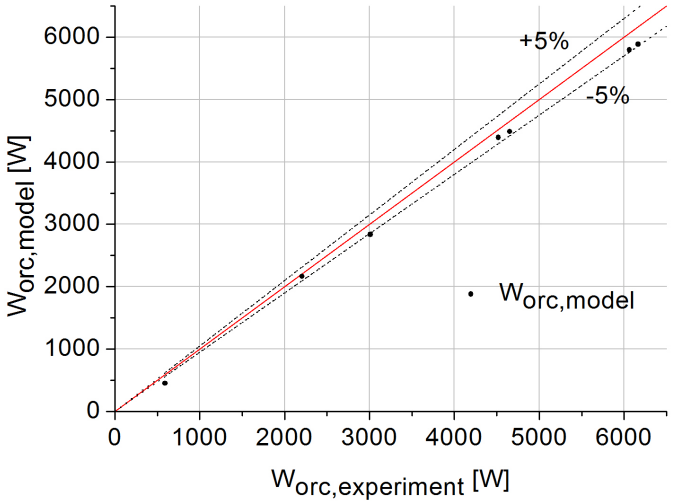

Figure 4: Prediction by the model of the eletrical output power

The model is able to reproduce the electrical power output with a 5% accuracy for most of the operating condition. For low power output the model predicts the experimental data with an accuracy of 20%.

6. CONCLUSION

In this paper the experimental characterization of a single screw expander in an ORC system, using Solkatherm as working fluid, for bottoming stationary waste heat recovery application is presented. The expander is obtained by modifying a single screw compressor to run in reverse and it is characterized by a built-in volume ratio of 6. Measured profile are collected for a wide range of working conditions. The maximum power is 7.8 kW at 3000 rpm and the expander isentropic efficiency reaches a peak value of 64.7% at 3000 rpm for a pressure ratio of 7.7, which is in line with the performance reported in Wang et al. (2013). A low-order semi-empirical model of the expander has been derived based on performance curves representing the expander isentropic efficiency and the group $\varphi \cdot V_s$. Empirical expressions for pump performance and pressure drops in the heat exchangers are also presented. Finally a steady-state model of the whole ORC system has been implemented by assembling the different component sub-models. The comparison between the overall model and the data reveals a maximum error of 5% for most of the points.

NOMENCLATURE

ORC Organic rankine cycle
WHR Waste heat recovery
APS Absolute pressure sensor
CFM Coriolis flow meter
RTD Resistance temperature detector
$\dot{m}$ Mass flow rate (kg/s)
$\dot{W}$ Power (W)
$\dot{V}$ Volume flow rate (m^3/s)
V Volume (m^3)
f Frequency (Hz)
N Rotational speed (rpm)
p Pressure (Pa)
T Temperature (°C)
h Specific enthalpy (J/kg)

Subscript
e Electric
ev Evaporator
ex Exhaust
exp Expander
HP High pressure
is Isentropic
LP Low pressure
p Pressure
P Pump
PP Pinch point
rot Rotational
s Swept
su Supply
T Thermal

Greek letter
ρ Density (kg/m^3)
φ Filling factor
η Efficiency
Δ Difference

REFERENCES

Angelino, G., Gaia, M., and Macchi, E. (1984). A review of italian activity in the field of organic rankine cycles. *Verein Deutscher Ingenieure Berichte 539*, pages 465--482.

Bell, I., Wronski, J., Quoilin, S., and Lemort, V. (2014). Pure- and Pseudo-Pure Fluid Thermophysical Property Evaluation and the Open-Source Thermophysical Property Library CoolProp.

David, G., Michel, F., and Sanchez, L. (2011). Waste heat recovery projects using organic rankine cycle technology examples of biogas engines and steel mills applications. In *Workd Engineers convention*.

Davidson, T. A. (1977). Design and analusis of a 1 kw rankine power cycle, employing a multi-vane expander, for use with a lox temperature solar collector. Master's thesis, Massachusetts Institute of Technology.

Declaye, S., Quoilin, S., Guillaume, L., and Lemort, V. (2013). Experimental study on an open-drive scroll expander integrated into an {ORC} (organic rankine cycle) system with {R245fa} as working fluid. *Energy*, 55(0):173 -- 183.

Desideri, A., van den B., M., Gusev, S., Lecompte, S., Lemort, V., and Quoilin, S. (2013). Experimental study and dynamic modeling of a whr orc power system with screw expander.

DOE (2008). Waste heat recovery: Technology and opportunites in u.s. industry. Technical report, U.S. Department of Energy Industrial technologies Program.

He, W., Wu, Y., Peng, Y., Zhang, Y., Ma, C., and Ma, G. (2013). Influence of intake pressure on the performance of single screw expander working with compressed air. *Applied Thermal Engineering*, 51(1–2):662 -- 669.

Huber, P. (1992). *Robust Statistics*. John Viley and Sons.

IEA (2010). Industrial Excess Heat Recovery Technologies & Applications. Technical report, Industrial Energy-related Technologies and Systems (IETS).

Lemort, V., Declaye, S., and Sylvain, Q. (2011). Experimental characterization of a hermetic scroll expander for use in a micro-scale rankine cycle. *Proccedings of the Institution of Mechanical Engineers, Part A: Journal of Power and Energy*, 226(1).

Mattsson, S. and Elmqvist, H. (April 28-30, 1997). Modelica - an international effort to design the next generation modeling language. In *7th IFAC Symposium on Computer Aided Control Systems Design, CACSD'97*.

Moynihan, P. I. (1982). Application guide for waste heat recovery with organic rankine cycle equipment. Technical report, Jet propulsion laboratory California Institute of Technology.

Persson, J. (1990). Performance mapping vs design parameters for screw compressors and other displacement compressor types. *Verein Deutscher Ingenieure Berichte 539*, 859:15 -- 31.

Quoilin, S. (October 2011). *Sustainable Energy Conversion Through the Use of Organic Rankine Cycles for Waste Heat Recovery and Solar Applications*. PhD thesis, University of Liege.

Quoilin, S., Declaye, S., Legros, A., Guillaume, L., and Vincent, L. (2012). Working fluid selection and operating maps for organic rankine cycle expansion machines. In *Proceedings of the 21st International Compressor Conference at Purdue*.

Quoilin, S., Van Den Broek, M., Declaye, S., Dewallef, P., and Lemort, V. (2013). Techno-economic survey of organic rankine cycle (orc) systems. *RENEWABLE & SUSTAINABLE ENERGY REVIEWS*, 22:168--186.

Sergei, G., Ziviani, D., Bell, I., De Paepe, M., and Van Den Broek, M. (2014). Experimental comparison of working fluids for organic rankine cycle with single-screw expander. In *15th International Refrigeration and Air Conditioning Conference. Paper 653*.

Verneau, A. (1979). Waste heat recovery by organic fluid rankine cycle. In *Proceedings from the First Industrial Energy Technology Conference Houston*.

Walraven, D., Laenen, B., and D'haeseleer, W. (2013). Comparison of thermodynamic cycles for power production from low-temperature geothermal heat sources. *Energy Conversion and Management*, 66(0):220 -- 233.

Wang, W., ting Wu, Y., fang Ma, C., ding Liu, L., and Yu, J. (2011). Preliminary experimental study of single screw expander prototype. *Applied Thermal Engineering*, 31(17–18):3684 -- 3688. {SET} 2010 Special Issue.

Wang, W., ting Wu, Y., fang Ma, C., dong Xia, G., and fu Wang, J. (2013). Experimental study on the performance of single screw expanders by gap adjustment. *Energy*, 62(0):379 -- 384.

Ziviani, D., Bell, I., Paepe, D., and M., van den Broek, M. (2014). Comprehensive model of a single screw expander for orc-systems applications. In *2014 Purdue Conferences: Compressor Engineering Refrigeration and air conditioning high performance building. Paper 506.*

ACKNOWLEDGEMENT

The results presented in this paper have been obtained within the frame of the IWT SBO-110006 project The Next Generation Organic Rankine Cycles (www.orcnext.be), funded by the Institute for the Promotion and Innovation by Science and Technology in Flanders. This financial support is gratefully acknowledged.